THE PROTEIN SOCIETY

Interaction of double-stranded DNA with polymerized PprA protein from *Deinococcus radiodurans*

Motoyasu Adachi,[1] Hiroshi Hirayama,[1] Rumi Shimizu,[1] Katsuya Satoh,[2] Issay Narumi,[2] and Ryota Kuroki[1]*

[1]Molecular Biology Research Division, Quantum Beam Science Center, Japan Atomic Energy Agency, Ibaraki 319-1195, Japan
[2]Medical and Biotechnological Application Division, Quantum Beam Science Center, Japan Atomic Energy Agency, Gunma 370-1292, Japan

Received 30 April 2014; Accepted 11 July 2014
DOI: 10.1002/pro.2519
Published online 15 July 2014 proteinscience.org

Abstract: Pleiotropic protein promoting DNA repair A (PprA) is a key protein that facilitates the extreme radioresistance of *Deinococcus radiodurans*. To clarify the role of PprA in the radioresistance mechanism, the interaction between recombinant PprA expressed in *Escherichia coli* with several double-stranded DNAs (i.e., super coiled, linear, or nicked circular dsDNA) was investigated. In a gel-shift assay, the band shift of supercoiled pUC19 DNA caused by the binding of PprA showed a bimodal distribution, which was promoted by the addition of 1 m*M* Mg, Ca, or Sr ions. The dissociation constant of the PprA-supercoiled pUC19 DNA complex, calculated from the relative portions of shifted bands, was 0.6 μ*M* with Hill coefficient of 3.3 in the presence of 1 m*M* Mg acetate. This indicates that at least 281 PprA molecules are required to saturate a supercoiled pUC19 DNA, which is consistent with the number (280) of bound PprA molecules estimated by the UV absorption of the PprA–pUC19 complex purified by gel filtration. This saturation also suggests linear polymerization of PprA along the dsDNA. On the other hand, the bands of linear dsDNA and nicked circular dsDNA that eventually formed PprA complexes did not saturate, but created larger molecular complexes when the PprA concentration was >1.3 μ*M*. This result implies that DNA-bound PprA aids association of the termini of damaged DNAs, which is regulated by the concentration of PprA. These findings are important for the understanding of the mechanism underlying effective DNA repair involving PprA.

Keywords: radiation; DNA repair; DNA binding; gel-shift assay; polymerization

Introduction

Deinococcus radiodurans is a eubacterium initially isolated from canned meat irradiated at 4000 Grays (Gy)[1] and was confirmed to exhibit a remarkable ability to recover from exposure to severe ionizing radiation and desiccation.[2–7] This extraordinary radioresistance is characterized by a D37 dose (radiation dose required to reduce survival to 37%) of 7000 Gy γ-rays.[8] *D. radiodurans* acquires 50- and 100-fold greater resistance to radiation than *Escherichia coli* during exponential and stationary growth phases, respectively.[3] Ionizing irradiation and desiccation cause DNA double-strand breaks (DSBs)[9,10]; thus, they are lethal to nearly all organisms. *D. radiodurans* can, however, survive >100 DSBs in their genomic DNA by irradiation with 5000 Gy,[11] whereas *E. coli* cannot live with only a few DSBs.[12]

Abbreviations: DSBs, DNA double-strand breaks; dsDNA, double-stranded DNA; Gy, Grays; kbp, kilobase pair; TA, Tris-acetate

Issay Narumi's current address is Department of Life Sciences, Toyo University, Gunma 374-0193, Japan

Grant sponsor: MEXT; Grant numbers: 19370046, 19380054.

*Correspondence to: Ryota Kuroki, Molecular Biology Research Division, Quantum Beam Science Center, Japan Atomic Energy Agency, 2–4 Shirakata-shirane, Tokai, Ibaraki 319-1195, Japan. E-mail: kuroki.ryota@jaea.go.jp

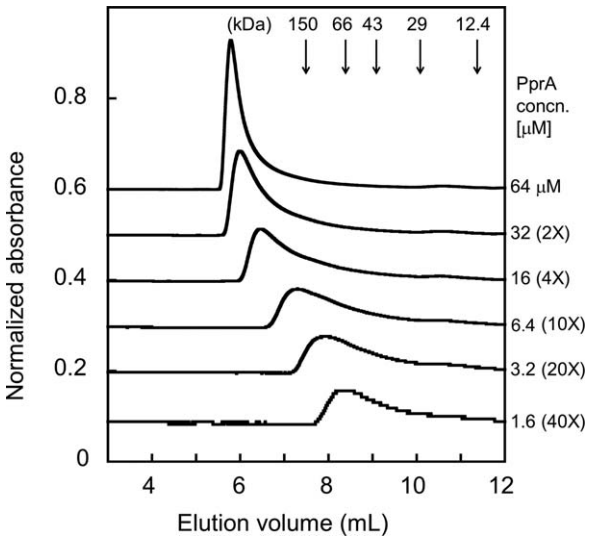

Figure 1. Effects of protein concentration on PprA self-association. Specified concentrations of PprA were applied to a TSKgel G3000SW$_{XL}$ gel filtration column, and the absorbance at 280 nm was plotted. Arrows indicate the elution volumes for alcohol dehydrogenase (150 kDa, 7.5 mL), bovine serum albumin (66 kDa, 8.4 mL), ovalbumin (43 kDa, 9.1 mL), carbonic anhydrase (29 kDa, 10.1 mL), and cytochrome *c* (12.4 kDa, 11.4 mL).

The genome sequence of *D. radiodurans* was determined in 1999.[13] *D. radiodurans* has genes coding for ~3200 proteins, including nearly all the homologous proteins involved in DNA repair in *E. coli* and about 1700 proteins of unknown function.[13] Molecular genetic analysis of DNA repair-deficient mutant strains has revealed three unique DSB repair proteins: pleiotropic protein promoting DNA repair A (PprA, *DRA0346*), inducer of PprA (PprI, *DR0167*), and modulator of PprA (PprM, *DR0907*).[14–16] PprI and PprM are positive and negative regulators, respectively, of PprA induction following irradiation. The induction of PprA is triggered by PprI-dependent post-translational modification of PprM.[16] It has also been shown that two other deinococcal regulatory proteins, LexA2 and RecX, suppress the expression of PprA.[17,18] Thus, PprA is a DNA repair protein that is induced in response to radiation stress in *D. radiodurans*.

PprA is a 32-kDa protein that does not show any significant amino acid similarity to other known proteins except PprAs from other members of the genus *Deinococcus*.[14,19–22] The reported molecular characteristics of PprA are as follows: PprA is induced when the bacterium is exposed to ionizing radiation[15,23–27]; PprA can bind to DNA[14,28]; PprA can promote the ligation activities of NAD-dependent *E. coli* DNA ligase and ATP-dependent T4 DNA ligase[14]; and PprA can inhibit DNA degradation by *E. coli* exonuclease III.[14] These characteristics suggest the possibility of a nonhomologous end joining repair pathway in *D. radiodurans*. Kota *et al.*[29] have reported the isolation of a multiprotein complex including PprA and an ATP-type DNA repair ligase. Additionally, PprA can stimulate catalase activity in *E. coli*[30] and contribute to genome maintenance.[31,32] Thus, PprA appears to be a potential pleiotropic protein that functions in the repair of DSBs and other radiation-induced damage. However, the molecular mechanism underlying DNA repair involving PprA remains unclear.

In this study, we demonstrate the characteristics of the interaction between several different DNAs and homogeneously purified recombinant PprA using gel filtration and gel-shift assays.

Results

Effects of protein and salt concentration on PprA self-association evaluated by gel filtration

Because alterations in the oligomeric state of PprA are thought to be related to its radioresistance, we analyzed the effects of PprA concentration on its self-association by gel filtration. Figure 1 shows the elution patterns of PprA from a gel filtration column. The injected PprA concentration ranged from 1.6 μ*M* (0.05 mg/mL) to 64 μ*M* (2.0 mg/mL). Owing to the viscosity of the protein solution, the elution patterns were not analyzed at concentrations above 64 μ*M*. The elution of PprA showed a peak with a

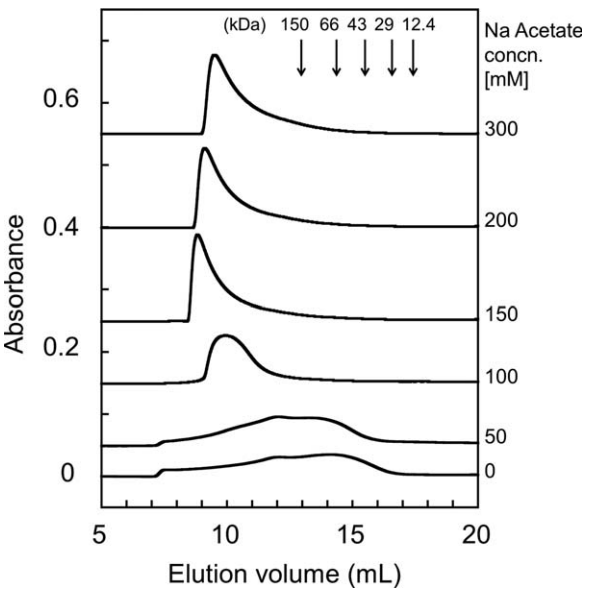

Figure 2. Effects of salt concentration on PprA self-association. A Superdex 200 10/300GL gel filtration column was equilibrated with TA buffer containing 0–300 m*M* Na acetate and 1 m*M* Mg acetate as indicated on the plot. The sample (0.05 mL) containing 32 μ*M* (1 mg/mL) PprA and TA buffer with 40 m*M* Na acetate and 1 m*M* Mg acetate was injected, and protein elution was monitored by measuring the absorbance at 280 nm. Arrows indicate the elution volumes of alcohol dehydrogenase (150 kDa, 12.9 mL), bovine serum albumin (66 kDa, 14.3 mL), ovalbumin (43 kDa, 15.4 mL), carbonic anhydrase (29 kDa, 16.5 mL), and cytochrome *c* (12.4 kDa, 17.3 mL).

broad tail, and the peak position drastically changed as the PprA concentration increased. With a 3.2 μ*M* (0.1 mg/mL) injection, the molecular mass of the major PprA fraction was estimated to be ~120 kDa, corresponding to a tetramer. The molecular weight of PprA increased significantly as the amount of injected PprA increased. With a 64 μ*M* (2.0 mg/mL) injection, the molecular mass of PprA, as determined by light scattering, increased to $\sim 3.0 \times 10^6$ kDa corresponding to a 100-mer. Therefore, the polymerization of PprA strongly depended on its concentration.

Because protein association is often affected by salt concentration, the characteristics of PprA self-association were further investigated by gel filtration at different salt concentrations using Tris-acetate (TA) buffer. Figure 2 shows the elution patterns of PprA in TA buffers containing 0, 50, 100, 150, 200, or 300 m*M* Na acetate. At the lower salt concentrations of 0 and 50 m*M*, the PprA elution was broadly distributed, indicating the elution of various complexes with different molecular weights. As the salt concentration increased, the major PprA peak was eluted earlier (shifted to higher molecular weights). The elution volume of PprA increased up to the salt concentration of 150 m*M*, and then it decreased slightly at 200 and 300 m*M* salt. PprA self-association depends on the salt concentration, and the highest polymeric state was observed at 150 m*M* Na acetate.

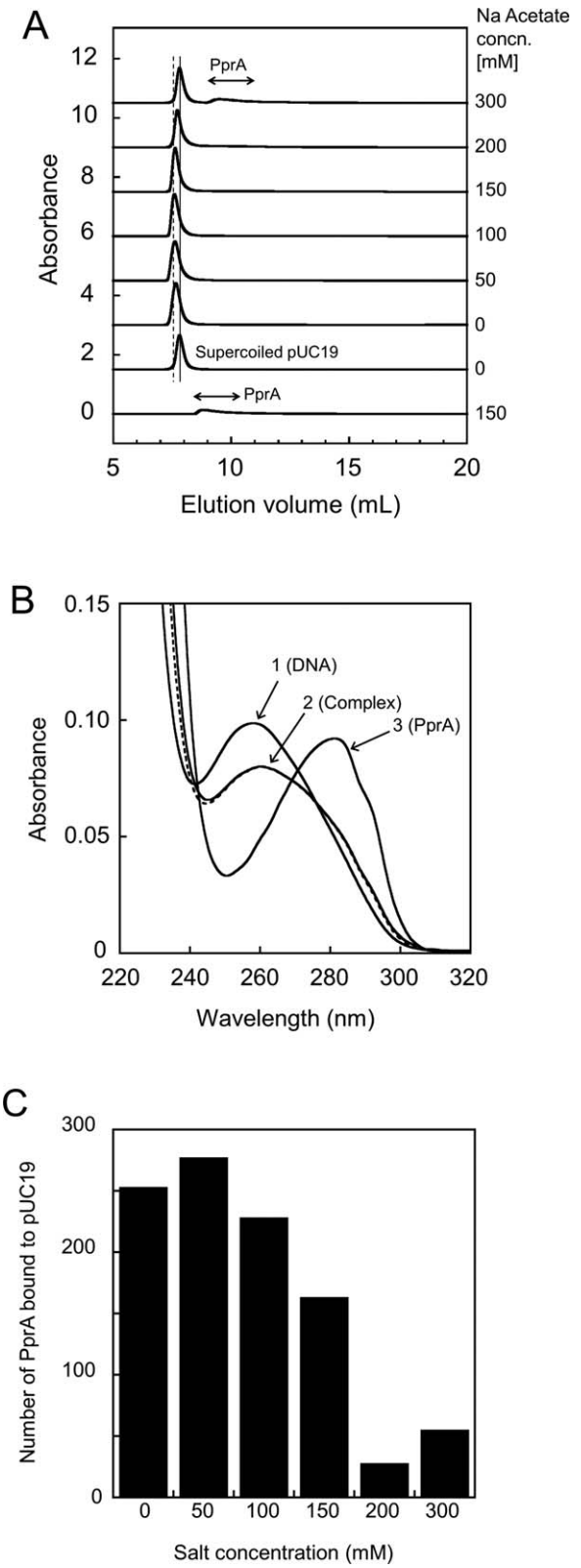

Figure 3. Isolation of PprA–DNA complexes. (A) A Superdex 200 10/300GL gel filtration column was equilibrated with TA buffer containing 1 m*M* Mg acetate and 0–300 m*M* Na acetate as indicated. The sample (0.05 mL) containing 32 μ*M* (1 mg/mL) PprA, 5.8 n*M* (0.01 mg/mL) supercoiled pUC19 DNA, and TA buffer with 40 m*M* Na acetate and 1 m*M* Mg acetate was injected. Uncomplexed DNA and protein are also shown. (B) UV spectral analyses of PprA, DNA, and PprA–DNA complexes. Supercoiled pUC19 DNA (1), PprA (2), and PprA–DNA complex (3) were eluted from the gel filtration column at 50 m*M* Na acetate as shown in (A). The dotted line indicates the curve calculated from the absorbance at 260 and 280 nm, in which the molar ratio of DNA to PprA was 1:280. (C) The molar ratios of DNA to PprA in the eluted samples in (A) were calculated as in (B) and plotted.

Effects of PprA and salt concentration on PprA–DNA association analyzed by gel filtration

To investigate the effect of salt concentration on PprA–DNA association, mixtures of double-stranded DNA (dsDNA) and PprA were examined by gel filtration. Supercoiled pUC19 (2686 bp, MW = 1.65×10^6) was used because its apparent molecular weight was sufficiently large to differentiate it from the unbound PprA.

In Figure 3(A), the elution patterns of PprA-supercoiled pUC19 mixtures are shown. The peak representing the PprA–DNA complex was slightly shifted to a lower elution volume (to a higher molecular weight) compared to that of supercoiled pUC19. The elution of the complex gradually shifted toward a higher molecular weight position as the Na acetate concentration increased up to 100 m*M*, and then gradually decreased at higher concentrations (150–300 m*M*) of Na acetate. In the presence of 300 m*M* Na acetate, the elution pattern of the PprA–DNA

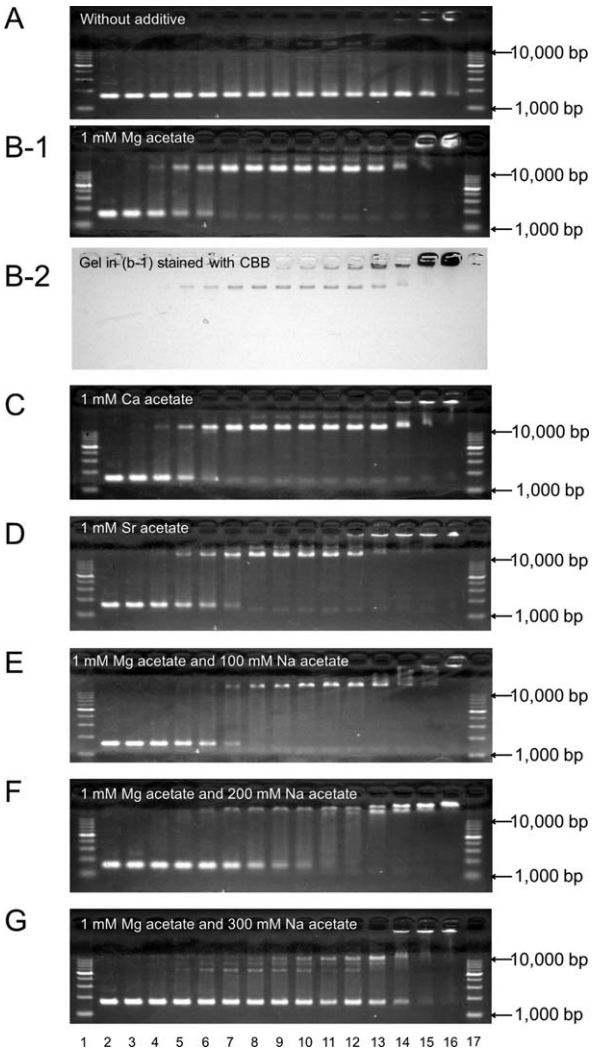

Figure 4. Effects of gel-shift assay conditions on the binding of PprA to DNA. Reaction mixtures containing 0.01 μg/mL DNA and varying amounts of PprA were applied to the wells of an agarose gel. Lanes 1 and 17, 1-kb DNA ladder markers; lane 2, 0 μ*M* (0 mg/mL); lane 3, 0.32 μ*M* (0.01 mg/mL); lane 4, 0.64 μ*M* (0.02 mg/mL); lane 5, 0.97 μ*M* (0.03 mg/mL); lane 6, 1.3 μ*M* (0.04 mg/mL); lane 7, 1.6 μ*M* (0.05 mg/mL); lane 8, 1.9 μ*M* (0.06 mg/mL); lane 9, 2.3 μ*M* (0.07 mg/mL); lane 10, 2.6 μ*M* (0.08 mg/mL); lane 11, 2.9 μ*M* (0.09 mg/mL); lane 12, 3.2 μ*M* (0.1 mg/mL); lane 13, 6.5 μ*M* (0.2 mg/mL); lane 14, 16 μ*M* (0.5 mg/mL); lane 15, 32 μ*M* (1.0 mg/mL); and lane 16, 64 μ*M* (2.0 mg/mL). The solutions in the electrophoresis chamber were in 1× TA buffer without additive (A), with 1 m*M* Mg acetate (B), with 1 m*M* Ca acetate (C), with 1 m*M* Sr acetate (D), with 1 m*M* Mg acetate and 100 m*M* Na acetate (E), with 1 m*M* Mg acetate and 200 m*M* Na acetate (F), and with 1 m*M* Mg acetate and 300 m*M* Na acetate (G).

complex was similar to that of supercoiled pUC19 alone.

To estimate the molecular ratio of PprA and supercoiled pUC19 in the peaks, the UV spectra of the peak fractions were measured. The UV spectra of PprA and pUC19 at 50 m*M* Na acetate are shown in Figure 3(B). From the relative absorbance of PprA and DNA at 260 and 280 nm, respectively, the number of PprA molecules bound to one supercoiled pUC19 molecule was calculated and plotted against salt concentration as shown in Figure 3(C). The largest number of PprA molecules bound to one supercoiled pUC19 was ~280 in the presence of 50 m*M* Na acetate. In this condition (50 m*M* Na acetate), the elution pattern of the complex was not altered even when twice the amount of PprA to DNA was used (data not shown). The number of PprA molecules bound to supercoiled pUC19 markedly decreased in the presence of Na acetate at concentrations above 200 m*M*.

Effect of metal ions on PprA–DNA association analyzed by gel-shift assays

As reported previously,[14] PprA binding to DNA can be detected by gel-shift assays. Because interactions between DNA and protein are often affected by divalent metal ions, the affinity of PprA for DNA in the presence of Mg, Ca, or Sr ions was determined by band shift experiments with 5.8 n*M* supercoiled pUC19 (0.01 μg/mL) and increasing PprA concentrations ranging from 0 to 64 μ*M* (0–2.0 mg/mL) as shown in Figure 4(A–G). Although the shift of the DNA by PprA was not observed in TA buffer without additives [Fig. 4(A)], in the presence of 1 m*M* Mg acetate, the DNA band was shifted from the position of 1500 bp to the position corresponding to 10,000 bp as the concentration of PprA increased [Fig. 4(B-1)].

To confirm the presence of PprA in the shifted DNA band, the agarose gel was stained with Coomassie Brilliant Blue (CBB) as shown in Figure 4(B-2). When the CBB-stained agarose gel was superimposed on the ethidium bromide-stained agarose gel, the locations of the PprA bands aligned with those of the shifted DNA bands, and the changes in the thickness of the PprA bands stained by CBB were similar to those of the DNA bands stained by ethidium bromide. When PprA was treated with 0.1% (w/v) sodium dodecyl sulfate at 37°C for 10 min, this DNA shift was not observed (data not shown). The bands in binding reactions with 1 m*M* Ca acetate [Fig. 4(C)] or 1 m*M* Sr acetate [Fig. 4(D)] were shifted similar to that with 1 m*M* Mg acetate [Fig. 4(B)].

In addition, the effect of salt concentration on recombinant PprA binding to DNA was investigated by changing the Na acetate concentration from 100 to 300 m*M* and the PprA concentration from 0 to 64 μ*M* (0–2.0 mg/mL) in the presence of 5.8 n*M* (0.01 mg/mL) supercoiled pUC19. The results are shown in Figure 4(E–G). Most of the DNA bands were shifted at a PprA concentration of 1.3 μ*M* (0.04 mg/mL, lane 6) with 1 m*M* Mg acetate [Fig. 4(B)], whereas the DNA band shifts occurred at higher PprA concentrations of 1.6, 2.6, and 16 μ*M* (0.05, 0.08, and 0.5 mg/mL; lanes 7, 10, and 14) in

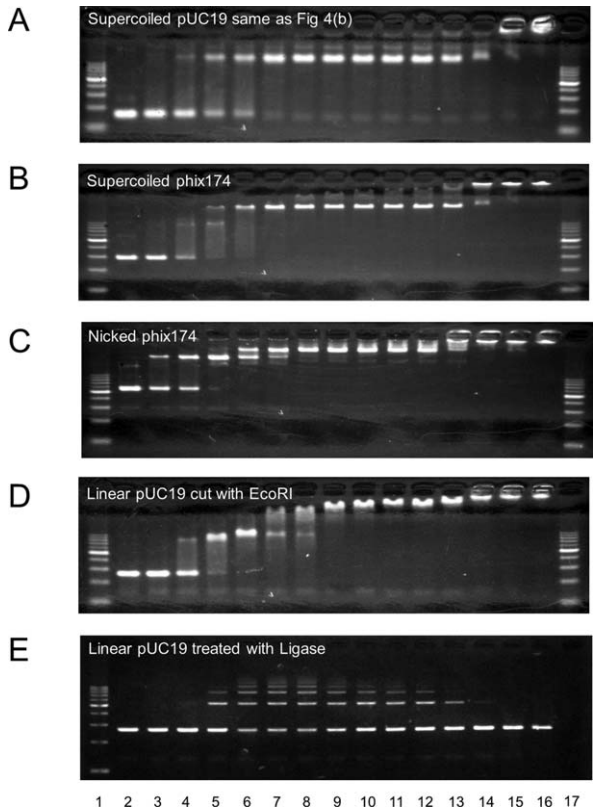

Figure 5. Gel-shift assays for the binding of PprA to DNA. Reaction mixtures containing 0.01 μg/mL DNA and varying amounts of PprA were applied to the wells of an agarose gel similar to that in Figure 4. (A) supercoiled pUC19 dsDNA, (B) supercoiled φX174 dsDNA, (C) nicked circular φX174 dsDNA, (D) pUC19 dsDNA linearized with *Eco*RI, (E) reaction mixtures of pUC19 dsDNA linearized with *Eco*RI in (D) were reacted with 0.035 U of ligase with 20 m*M* ATP at 37°C for 10 min, and loaded onto the gel after the addition of SDS at a final concentration of 0.1% (w/v).

100, 200, and 300 m*M* Na acetate, respectively. The size of the shifted DNA in 300 m*M* Na acetate was smaller than those in 100 and 200 m*M* Na acetate. Although all the DNA penetrated into the agarose gel in 200 m*M* Na acetate [Fig. 4(E,F)], the DNA was stacked near the well in the presence of 16, 32, and 64 μ*M* PprA (0.5, 1.0, and 2.0 mg/mL, lanes 14–16) in 300 m*M* Na acetate [Fig. 4(G)].

Effect of DNA shape on PprA–DNA association analyzed by gel-shift assays

To investigate the effect of the shape and length of DNA on the binding of PprA, gel-shift assays were performed using supercoiled dsDNA, linear dsDNA, and nicked circular dsDNA with various PprA concentrations.

With the supercoiled dsDNAs, pUC19 (2686 bp) and φX174 RFI (5386 bp), a bimodal distribution between shifted and nonshifted bands was observed [Fig. 5(A,B)]. In both cases, the band shift began at PprA concentrations of 0.64–0.97 μ*M* (0.02–0.03 mg/mL, lanes 4–5), and the DNA was shifted to a certain molecular size (>10,000 bp) as shown in Figure 5(A,B). When the concentration of PprA increased to >16 μ*M* (lane 14), pUC19 did not fully penetrate the gel.

When nicked circular dsDNA (φX174 RFII) was used, the position of the DNA began to shift at 0.32 μ*M* PprA (0.01 mg/mL, lane 3). Two shifts were observed at increasing PprA concentrations, with the second shift starting at a PprA concentration of 1.3 μ*M* (0.04 mg/mL, Lane 6) [Fig. 5(C)]. When linear dsDNA was used (supercoiled pUC19 cut with *Eco*RI), the position of the DNA shifted to 8 kbp at 0.64 μ*M* PprA (0.02 mg/mL, lane 4) and gradually increased toward a higher molecular weight at higher PprA concentrations [Fig. 5(D)]. The band of linear dsDNA was completely shifted in the presence of 1.3 μ*M* PprA (0.04 mg/mL, lane 6), and the band was further shifted to a larger size (>10,000 bp) PprA–DNA complex in the presence of 1.6 μ*M* PprA (0.05 mg/mL, lane 7). It appears that PprA somehow distinguishes the termini of nicked circular dsDNA and linear dsDNA from supercoiled dsDNA, resulting in a secondary shift of a larger molecular size.

Effect of DNA size on PprA–DNA association analyzed by gel-shift assays

To investigate the influence of DNA size on PprA binding, PprA binding to DNA was characterized by gel-shift assays using three sets of DNA ladder markers containing different sized dsDNA fragments at different PprA concentrations. Upon addition of PprA to the mixture of DNA fragments (100-bp ladder DNA) at sizes ranging from 0.1 to 1.0 kbp, the DNA was widely distributed as a smeared band, and a part of the complex was stacked at the bottom of the wells [Fig. 6(A)]. The DNA shift began at a PprA concentration of 0.32 μ*M* (0.01 mg/mL, lane 3). In the lanes containing PprA at concentrations of 0.32–0.97 μ*M* (0.01–0.03 mg/mL, lanes 3–5), it appeared that PprA preferentially recognized the higher molecular-sized DNAs rather than the lower molecular-sized DNAs. In the presence of 64 μ*M* PprA (2 mg/mL, lane 16), the band shift was observed even with 200 bp of linear dsDNA.

To identify the minimum size of DNA shifted by PprA, two sets of smaller DNA markers, a low-molecular-weight DNA ladder containing 25–766 bp fragments (lanes 1–4) and a 10-bp DNA step ladder containing 10–100 bp fragments (lanes 5–8), were used in the gel-shift assay [Fig. 6(B)]. DNAs that were >200 bp were shifted at higher PprA concentrations; however, the shift was not observed when the DNA was <150 bp in length and when the 10-bp DNA step ladder was used [Fig. 6(B), lanes 1–4].

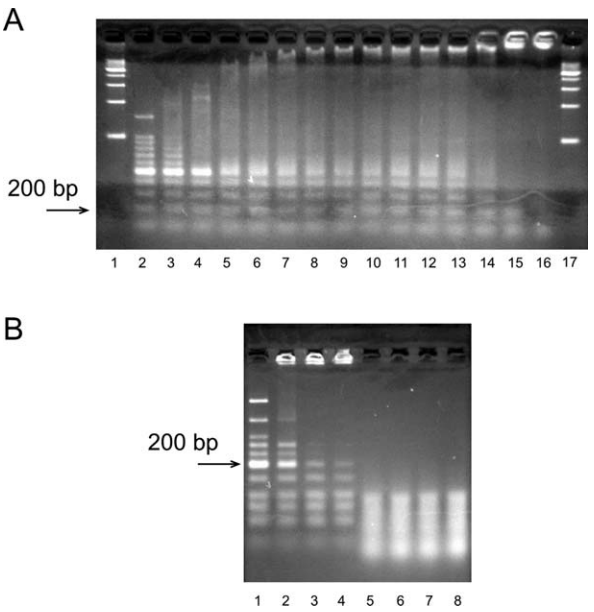

Figure 6. Gel-shift assays for the binding of PprA to mixtures of smaller DNAs. (A) A 100-bp ladder was used as the DNA, and the PprA concentrations were varied as in Figure 4. Reaction mixtures (10 μL) containing 0.13 μg of DNA were applied to the wells of a 2% agarose gel. In lanes 1 and 17, the 1-kb DNA ladder marker was loaded. (B) Reaction mixtures (10 μL) containing 0.5 μg of the low-molecular-weight DNA ladder and the 10-bp DNA step ladder with the following PprA concentrations were applied to the wells of a 4% agarose gel: lanes 1 and 5, 0 μ*M* (0 mg/mL); lanes 2 and 6, 16 μ*M* (0.5 mg/mL); lanes 3 and 7, 32 μ*M* (1.0 mg/mL); lanes 4 and 8, 64 μ*M* (2.0 mg/mL). Nusieve 3:1 agarose was used to prepare the gels.

Effect of PprA concentration on the ligation reaction

To understand the effect of PprA concentration on the ligation reaction, a mixture containing PprA and linear DNA was reacted with ligase, and the size of the oligomer was analyzed by electrophoresis after denaturation of PprA [Fig. 5(E)]. A ligated dimer of DNA with a size of 5 kbp was faintly observed at 0.64 μ*M* PprA (0.02 mg/mL, lane 4), and was obvious at PprA concentrations ranging from 0.97 μ*M* (0.03 mg/mL, lane 5) to 6.5 μ*M* (0.2 mg/mL, lane 13). The ligation reaction was effectively facilitated by PprA concentrations ranging from 1.3 μ*M* (0.04 mg/mL, lane 6) to 2.3 μ*M* (0.07 mg/mL, lane 9), where a pentamer of DNA with a size of 10 kbp was slightly observed. Ligation of DNA was gradually inhibited at increasing PprA concentrations, and it was strongly inhibited at >16 μ*M* (0.5 mg/mL, lane 14) although a higher order PprA–DNA complex was formed [Fig. 5(D), lanes 15 and 16].

Discussion

To understand the unique mechanism of radioresistance in *D. radiodurans*, the interaction between DNA and homogeneously purified recombinant PprA was characterized by gel filtration and gel-shift assays. We first focused on the characteristics of PprA self-association because previous gel filtration results suggested that PprA forms 12-mers, whereas the results with atomic force microscopy indicated that PprA monomers or dimers could bind to DNA.[28] These inconsistencies might be due to differences in the experimental conditions, such as the protein concentration, because the self-association of PprA without DNA significantly depends on the PprA and salt concentrations, as shown in Figures 1 and 2. In addition, it is considered that the large change in molecular weight as PprA concentration increases is important for its function as a pleiotropic protein, because PprA expression is induced following exposure to ionizing radiation.[15,23–27] It is also considered that the ability of PprA to form higher molecular weight entities is responsible for the extraordinary radioresistance of *D. radiodurans*.

Next, we focused on the DNA-binding characteristics of PprA. We investigated the influence of protein concentration on the DNA binding of PprA by using a gel-shift assay because large shifts of DNA were previously reported using gel-shift assays.[14] Band shifts were observed when using supercoiled pUC19 and φX174-lacking ends or nicks [Fig. 5(A,B)] and were also observed with ladder markers comprising several sizes of DNA fragments (Fig. 6), suggesting that PprA binding to DNA does not depend on the DNA sequence. In addition, PprA binding requires a DNA molecule that is >200 bp [Fig. 6(B)], which may be the minimum size of DNA required for PprA binding.

Moreover, the DNA binding of PprA was strongly dependent on the presence of divalent alkali earth metal ions and was influenced by salt concentrations of 0.1–0.3*M*. These results suggest that divalent ions promote DNA–PprA interaction, and that electrostatic interactions play a key role in the DNA binding of PprA. Given that PprA binding to DNA is independent of the DNA sequence, polymerized PprA probably forms a nucleoprotein with DNA and recognizes the phosphate and deoxyribose backbone.

The bimodal distribution of supercoiled pUC19 DNA with and without PprA binding can provide important information about the dissociation constant (K_d) between PprA and DNA. The DNA shift was estimated densitometrically from the thickness of the bands, and was plotted against PprA concentration, as shown in Figure 7. The plot shows K_d value of 0.60 μ*M* (0.02 mg/mL) and Hill coefficient of 3.3 for the binding of PprA to supercoiled pUC19. The DNA-binding characteristics of PprA dramatically changed at a concentration of ~1 μ*M* PprA as a result of cooperativity. We speculate that this cooperative change would make it possible to regulate the

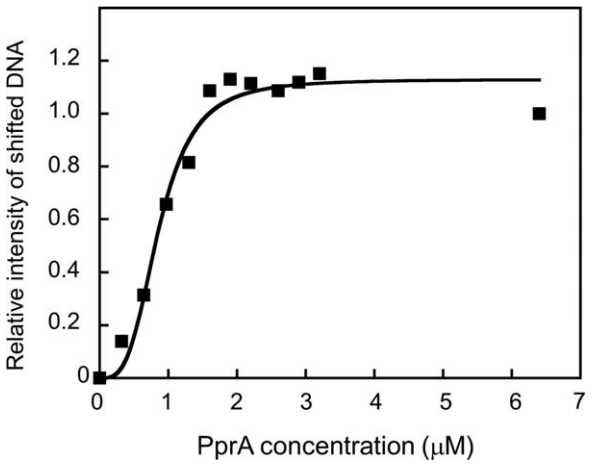

Figure 7. Binding curve for polymerized PprA binding to supercoiled pUC19. The amount of supercoiled pUC19 complexed with PprA, as illustrated in Figure 4B-1, was estimated densitometrically and plotted. For normalization, the amount was divided by the value of pUC19 in Figure 4B-1, lane 2. The data were fit to a previously reported equation[33] using KaleidaGraph.

effective DNA repairing by the radiation-induced expression of PprA. In addition, we estimated that 281 molecules of PprA bind to a molecule of supercoiled pUC19 (2686 bp) because the binding of PprA was saturated at 1.6 μ*M* (0.05 mg/mL) PprA in the presence of 5.8 n*M* supercoiled pUC19 [Fig. 7]. The calculated number of 281 was in agreement with the number (280 molecules) estimated from the UV spectrum of the PprA–pUC19 complex eluted from gel filtration.

Thus, it is now clear that ~280 molecules of PprA can bind to a molecule of supercoiled pUC19. Assuming that PprA is spherical, the diameter of PprA is estimated to be 40 Å using the value of the specific volume of 0.73 cm^3/g,[34] whereas the length of 9.6 bp of B-type DNA is equivalent to ~34 Å. This difference between 40 and 34 Å suggests that PprA linearly polymerizes along the DNA and forms a DNA–PprA complex with different pitches, such as helical-shaped oligomers, as shown in Figure 8(A), which is similar to that observed for DNA in complex with RecA.[35]

Based on these observations, the contribution of PprA in DSB repair is summarized in Figure 8(B). After radiation-induced DSBs, PprA expression is enhanced, which results in increased PprA concentration in the cell. This increase further assists the polymerization and formation of nucleoproteins with the damaged DNA. When the PprA concentration reaches 1.6 μ*M* (0.05 mg/mL), PprA facilitates linear dsDNA association as the terminal end of the cleaved DNA approaches the other terminal end of a different DNA located along with PprA because the secondary band shift of linear dsDNA was observed between 1.3 and 1.6 μ*M* PprA differently from bimodal distribution of supercoiled DNA [Fig. 5(A,D)]. This mechanism was partly supported by the fact that the optimum concentration of PprA facilitating the ligation reaction upon subcloning is 1.6 μ*M*[14] and oligomer formation of DNA ranged from 1.3 to 2.3 μ*M* [Fig. 5(E), lanes 6–9], corresponding to the optimum concentration required for the binding of PprA to DNA. However, further increase in PprA concentration rather inhibits the ligation reaction as shown in Figure 5(E), which prevented the association of the terminal ends of cleaved DNA owing to the excess amount of PprA.

Moreover, the results of the experiments on the interaction between PprA and several dsDNAs with different shapes provide important information on how PprA helps to repair damaged DNA. When linear and nicked circular dsDNAs were used, the distribution of the PprA–DNA complex was not bimodal; however, the PprA concentration required to initiate the band shift was similar, despite the differences in the topology of DNA, as shown in Figure 5. Interestingly, the bands further shifted to larger molecular sizes at increasing PprA concentrations. These results suggest that PprA can distinguish linear dsDNA and nicked circular dsDNA from supercoiled dsDNA by recognizing DNA termini. This intriguing discriminatory mechanism could explain the efficient repair of damaged DNA,

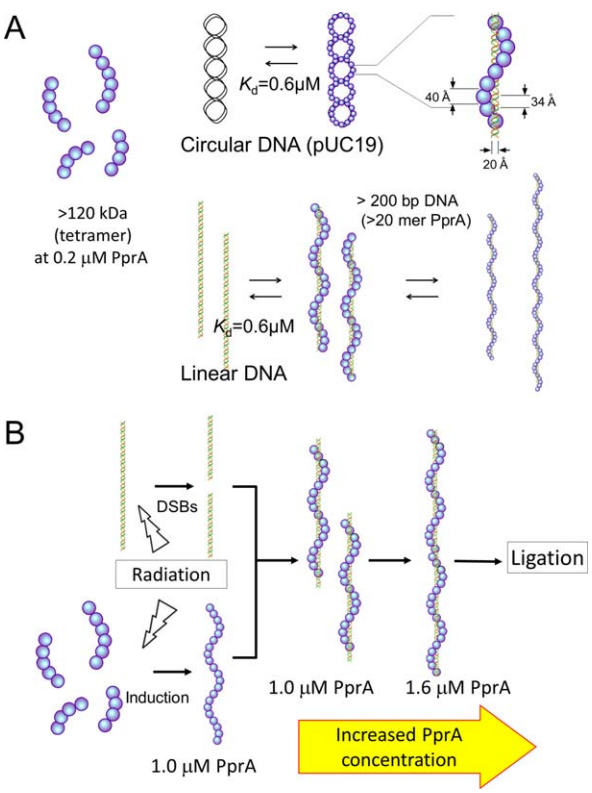

Figure 8. Schematic model of the ligation reaction of polymerized PprA complexed with DNA. PprA is depicted as spheres with diameters of 40 Å. The affinity between PprA molecules can stimulate the reaction catalyzed by ligase. (A) Model for the binding of PprA to circular and linear DNAs. (B) Proposed mechanism underlying DNA repair by PprA.

and it suggests the involvement of polymerized PprA in homologous recombination with RecA and/or in extended synthesis-dependent strand annealing.[36] The results that the PprA polymerization and the PprA–DNA interaction are regulated by the PprA concentration provide important insights into the mechanism underlying effective DNA repair involving PprA.

Materials and Methods

Materials

The 1-kb DNA ladder was composed of 10 DNA fragments (1, 2, 3, 4, 5, 6, 7, 8, 9, and 10 kbp; Takara Bio). The 100-bp DNA ladder (Takara Bio) was composed of 11 DNA fragments (0.1, 0.2, 0.3, 0.4, 0.5, 0.6, 0.7, 0.8, 0.9, 1.0, and 1.5 kbp). The low-molecular-weight DNA ladder (New England Biolabs) was composed of 11 DNA fragments (25, 50, 75, 100, 150, 200, 250, 300, 350, 500, and 766 bp). The 10-bp DNA step ladder (Promega) was composed of 10 DNA fragments (10, 20, 30, 40, 50, 60, 70, 80, 90, and 100 bp). The underlined DNA fragments indicate the thicker bands. SeaKem GTG Agarose and Nusieve 3:1 Agarose (Takara Bio) were used to prepare agarose gels for the separation of higher and lower molecular weight DNA fragments, respectively. φX174 RFI (5386 bp) and its nicked form φX174 RFII were purchased from New England Biolabs. Supercoiled pUC19 DNA was isolated from the transformants of *E. coli* strain JM109 with a QIAprep Spin Miniprep Kit (Qiagen) and linearized with *Eco*RI (Takara Bio).

PprA expression

The gene encoding PprA was subcloned into a pET vector carrying the kanamycin resistance gene using the following method. The expression plasmid pET3p-prAwt[14] containing the *pprA* gene was cut with *Nde*I and *Bam*HI. The generated 0.9-kbp fragment was inserted between the *Nde*I and *Bam*HI sites of the expression vector pET9a (Novagen). The resultant expression plasmid was designated pET9pprAwt, and was used to transform *E. coli* strain BL21(DE3) pLysS (Merck). Transformed *E. coli* were grown at 37°C in an 8 L of Luria-Bertani medium containing 30 μg/mL kanamycin and 35 μg/mL chloramphenicol, using a 10-L jar fermenter (Takasaki Scientific Instruments). When the optical density at 660 nm reached 1.0, isopropyl-β-D-thiogalactopyranoside was added to the medium to a final concentration of 0.4 m*M*. Growth was allowed to continue for an additional 5 h at 37°C. The cells were harvested by centrifugation for 20 min at 4500 rpm in a J6 MI centrifuge with fixed angle rotor JLA8.1000 (Beckman Coulter).

Purification of PprA

The cell pellets were resuspended in 1 L of lysis buffer [20 m*M* Tris-HCl [pH 8.0], 500 m*M* NaCl, 1 m*M* ethylenediaminetetraacetic acid, and 0.2 m*M* 4-(2-aminoethyl)benzenesulfonyl fluoride hydrochloride (Roche Applied Science)]. The cell suspension was sonicated, and the supernatant was collected by centrifugation for 15 min at 14,000 rpm in a Himac CR-21 centrifuge and fixed angle rotor R19A (Hitachi Koki) at 4°C. The resultant crude extract was fractionated with a 35% saturated ammonium sulfate solution. The supernatant was collected by centrifugation for 15 min at 14,000 rpm, and was applied to a Toyopearl Phenyl-650M column (25 mm × 100 mm; Tosoh) previously equilibrated with 50 m*M* sodium phosphate buffer (pH 6.5) containing 30% saturated ammonium sulfate. Proteins were eluted with a descending gradient of 30–0% ammonium sulfate. The fractions containing PprA were pooled and dialyzed against 20 m*M* Tris-HCl buffer (pH 8.0). After dialysis, the protein solution was applied to a HiLoad 26/10 Q Sepharose HP column (GE Healthcare). Proteins were eluted with a linear gradient of 0–500 m*M* NaCl in 20 m*M* Tris-HCl (pH 8.0). Fractions containing PprA were then dialyzed against 20 m*M* Tris-HCl buffer (pH 8.0) containing 100 m*M* NaCl. The protein solution was applied to an Affi-Gel Heparin Gel column (25 mm × 80 mm; BioRad). Proteins were eluted with a linear gradient of 100–500 m*M* NaCl in 20 m*M* Tris-HCl (pH 8.0). The purified PprA was dialyzed against 20 m*M* Tris-HCl buffer (pH 8.0) containing 200 m*M* Na acetate, and was concentrated to 160 μ*M* (5.0 mg/mL) with a Centriprep YM-10 (Millipore). The purity of the recombinant PprA was verified by SDS-PAGE analysis.

Gel filtration of PprA

PprA was injected onto a column (TSKgel G3000SW$_{XL}$, 7.8 mm I.D. × 300 mm; Tosoh) equilibrated with TA buffer (39 m*M* Tris base, 20 m*M* Na acetate, and 29 m*M* acetic acid) containing 200 m*M* Na acetate at a flow rate of 1.0 mL/min. PprA was diluted with 20 m*M* Tris-HCl buffer (pH 8.0) containing 200 m*M* Na acetate and injected in a volume of 0.05 mL. The elution of PprA protein was monitored using both the refractive index and UV detectors. The molecular mass of eluted PprA was determined by multiangle laser light scattering (SEC-MALLS). Light-scattering analysis was performed using a miniDAWN detector (Wyatt Technologies).

PprA and the DNA–PprA complex were injected onto a Superdex 200 10/300GL column (GE Healthcare) equilibrated with TA buffer containing 0–300 m*M* Na acetate and 1 m*M* Mg acetate at a flow rate of 0.75 mL/min.

Gel-shift assay for the binding of DNA to PprA

Reactions were initiated by the addition of PprA and incubated for 10 min at 37°C in 20 μL of TA buffer

with 1 m*M* Mg acetate and DNA. After incubation, the reactions were mixed with 4 μL of loading buffer containing 0.01% bromophenol blue, 10% (w/v) glycerol, and TA buffer, and subjected to agarose gel electrophoresis on 0.8% (w/v) GTG Agarose gels at 50 V. The electrophoresis was carried out using a Mupid submarine electrophoresis system (Advance). Agarose gels were stained with ethidium bromide.

Acknowledgment

The authors thank Enago (www.enago.jp) for English language review of the manuscript.

References

1. Anderson AW, Nordan HC, Cain RF, Parrish G, Duggan D (1956) Studies on radioresistant micrococcus. I. Isolation, morphology, cultural characteristics and resistance to gamma radiation. Food Technol 10: 575–582.
2. Battista JR (1997) Against all odds: the survival strategies of *Deinococcus radiodurans*. Annu Rev Microbiol 51:203–224.
3. Makarova KS, Aravind L, Wolf YI, Tatusov RL, Minton KW, Koonin EV, Daly MJ (2001) Genome of the extremely radiation-resistant bacterium *Deinococcus radiodurans* viewed from the perspective of comparative genomics. Microbiol Mol Biol Rev 65:44–79.
4. Narumi I (2003) Unlocking radiation resistance mechanisms: still a long way to go. Trends Microbiol 11:422–425.
5. Cox MM, Battista JR (2005) *Deinococcus radiodurans*—the consummate survivor. Nat Rev Microbiol 3: 882–892.
6. Blasius M, Sommer S, Hübscher U (2008) *Deinococcus radiodurans*: what belongs to the survival kit? Crit Rev Biochem Mol Biol 43:221–238.
7. Slade D, Radman M (2011) Oxidative stress resistance in *Deinococcus radiodurans*. Microbiol Mol Biol Rev 75: 133–191.
8. Moseley BE, Copland HJ (1975) Isolation and properties of a recombination-deficient mutant of *Micrococcus radiodurans*. J Bacteriol 121:422–428.
9. Dean CJ, Feldschreiber P, Lett JT (1966) Repair of x-ray damage to the deoxyribonucleic acid in *Micrococcus radiodurans*. Nature 209:49–52.
10. Mattimore V, Battista JR (1996) Radioresistance of *Deinococcus radiodurans*: functions necessary to survive ionizing radiation are also necessary to survive prolonged desiccation. J Bacteriol 178:633–637.
11. Moseley BE, Mattingly A (1971) Repair of irradiated transforming deoxyribonucleic acid in wild type and a radiation-sensitive mutant of *Micrococcus radiodurans*. J Bacteriol 105:976–983.
12. Krasin F, Hutchinson F (1977) Repair of DNA double-strand breaks in *Escherichia coli*, which requires recA function and the presence of a duplicate genome. J Mol Biol 116:81–98.
13. White O, Eisen JA, Heidelberg JF, Hickey EK, Peterson JD, Dodson RJ, Haft DH, Gwinn ML, Nelson WC, Richardson DL, Moffat KS, Qin H, Jiang L, Pamphile W, Crosby M, Shen M, Vamathevan JJ, Lam P, McDonald L, Utterback T, Zalewski C, Makarova KS, Aravind L, Daly MJ, Minton KW, Fleischmann RD, Ketchum KA, Nelson KE, Salzberg S, Smith HO, Venter JC, Fraser CM (1999) Genome sequence of the radioresistant bacterium *Deinococcus radiodurans* R1. Science 286:1571–1577.
14. Narumi I, Satoh K, Cui S, Funayama T, Kitayama S, Watanabe H (2004) PprA: a novel protein from *Deinococcus radiodurans* that stimulates DNA ligation. Mol Microbiol 54:278–285.
15. Hua Y, Narumi I, Gao G, Tian B, Satoh K, Kitayama S, Shen B (2003) PprI: a general switch responsible for extreme radioresistance of *Deinococcus radiodurans*. Biochem Biophys Res Commun 306:354–360.
16. Ohba H, Satoh K, Sghaier H, Yanagisawa T, Narumi I (2009) Identification of PprM: a modulator of the PprI-dependent DNA damage response in *Deinococcus radiodurans*. Extremophiles 13:471–479.
17. Satoh K, Ohba H, Sghaier H, Narumi I (2006) Down-regulation of radioresistance by LexA2 in *Deinococcus radiodurans*. Microbiology 152:3217–3226.
18. Sheng D, Jao J, Li M, Xu P, Zhang J (2009) RecX is involved in the switch between DNA damage response and normal metabolism in *D*. radiodurans. J Biochem 146:337–342.
19. Makarova KS, Omelchenko MV, Gaidamakova EK, Matrosova VY, Vasilenko A, Zhai M, Lapidus A, Copeland A, Kim E, Land M, Mavromatis K, Pitluck S, Richardson PM, Detter C, Brettin T, Saunders E, Lai B, Ravel B, Kemner KM, Wolf YI, Sorokin A, Gerasimova AV, Gelfand MS, Fredrickson JK, Koonin EV, Daly MJ (2007) *Deinococcus geothermalis*: the pool of extreme radiation resistance genes shrinks. PLoS One 2:e955.
20. de Groot A, Dulermo R, Ortet P, Blanchard L, Guérin P, Fernandez B, Vacherie B, Dossat C, Jolivet E, Siguier P, Chandler M, Barakat M, Dedieu A, Barbe V, Heulin T, Sommer S, Achouak W, Armengaud J (2009) Alliance of proteomics and genomics to unravel the specificities of Sahara bacterium *Deinococcus deserti*. PLoS Genet 5:e1000434.
21. Pukall R, Zeytun A, Lucas S, Lapidus A, Hammon N, Deshpande S, Nolan M, Cheng JF, Pitluck S, Liolios K, Pagani I, Mikhailova N, Ivanova N, Mavromatis K, Pati A, Tapia R, Han C, Goodwin L, Chen A, Palaniappan K, Land M, Hauser L, Chang YJ, Jeffries CD, Brambilla EM, Rohde M, Göker M, Detter JC, Woyke T, Bristow J, Eisen JA, Markowitz V, Hugenholtz P, Kyrpides NC, Klenk HP (2011) Complete genome sequence of *Deinococcus maricopensis* type strain (LB-34). Stand Genomic Sci 4:163–172.
22. Yuan M, Chen M, Zhang W, Lu W, Wang J, Yang M, Zhao P, Tang R, Li X, Hao Y, Zhou Z, Zhan Y, Yu H, Teng C, Yan Y, Ping S, Wang Y, Lin M (2012) Genome sequence and transcriptome analysis of the radioresistant bacterium *Deinococcus gobiensis*: insights into the extreme environmental adaptations. PLoS One 7: e34458.
23. Lipton MS, Pasa-Tolić L, Anderson GA, Anderson DJ, Auberry DL, Battista JR, Daly MJ, Fredrickson J, Hixson KK, Kostandarithes H, Masselon C, Markillie LM, Moore RJ, Romine MF, Shen Y, Stritmatter E, Tolić N, Udseth HR, Venkateswaran A, Wong KK, Zhao R, Smith RD (2002) Global analysis of the *Deinococcus radiodurans* proteome by using accurate mass tags. Proc Natl Acad Sci USA 99:11049–11054.
24. Liu Y, Zhou J, Omelchenko MV, Beliaev AS, Venkateswaran A, Stair J, Wu L, Thompson DK, Xu D, Rogozin IB, Gaidamakova EK, Zhai M, Makarova KS, Koonin EV, Daly MJ (2003) Transcriptome dynamics of *Deinococcus radiodurans* recovering from ionizing radiation. Proc Natl Acad Sci USA 100:4191–4196.

25. Ohba H, Satoh K, Yanagisawa T, Narumi I (2005) The radiation responsive promoter of the *Deinococcus radiodurans pprA* gene. Gene 363:133–141.
26. Zhang C, Wei J, Zheng Z, Ying N, Sheng D, Hua Y (2005) Proteomic analysis of *Deinococcus radiodurans* recovering from γ-irradiation. Proteomics 5:138–143.
27. Basu B, Apte SK (2011) Gamma radiation-induced proteome of *Deinococcus radiodurans* primarily targets DNA repair and oxidative stress alleviation. Mol Cell Proteomics 11:M111.011734.
28. Murakami M, Narumi I, Satoh K, Furukawa A, Hayata I (2006) Analysis of interaction between DNA and *Deinococcus radiodurans* PprA protein by atomic force microscopy. Biochim Biophys Acta 1764:20–23.
29. Kota S, Kamble VA, Rajpurohit YS, Misra HS (2010) ATP-type DNA ligase requires other proteins for its activity in vitro and its operon components for radiation resistance in *Deinococcus radiodurans* in vivo. Biochem Cell Biol 88:783–790.
30. Kota S, Misra HS (2006) PprA: a protein implicated in radioresistance of *Deinococcus radiodurans* stimulates catalase activity in *Escherichia coli*. Appl Microbiol Biotechnol 72:790–796.
31. Devigne A, Mersaoui S, Bouthier-de-la-Tour C, Sommer S, Servant P (2013) The PprA protein is required for accurate cell division of γ-irradiated *Deinococcus radiodurans* bacteria. DNA Repair 12: 265–272.
32. Kota S, Charaka VK, Ringgaard S, Waldor MK, Misra HS (2014) PprA contributes to *Deinococcus radiodurans* resistance to nalidixic acid, genome maintenance after DNA damage and interacts with deinococcal topoisomerases. PLoS One 9:e85288.
33. Grove A, Wilkinson SP (2005) Differential DNA binding and protection by dimeric and dodecameric forms of the ferritin homolog Dps from *Deinococcus radiodurans*. J Mol Biol 347:495–508.
34. Harpaz Y, Gerstein M, Chothia C (1994) Volume changes on protein folding. Structure 2:641–649.
35. Chen Z, Yang H, Pavletich NP (2008) Mechanism of homologous recombination from the RecA-ssDNA/dsDNA structures. Nature 453:489–494.
36. Zahradka K, Slade D, Bailone A, Sommer S, Averbeck D, Petranovic M, Lindner AB, Radman M (2006) Reassembly of shattered chromosomes in *Deinococcus radiodurans*. Nature 443:569–573.